Danish Meteorological Institute
Ministry of Transport

Scientific Report 04-07

Rotation of the surface stress as a tool in parameterization of atmospheric turbulence

Niels Woetmann Nielsen and Bent H. Sass

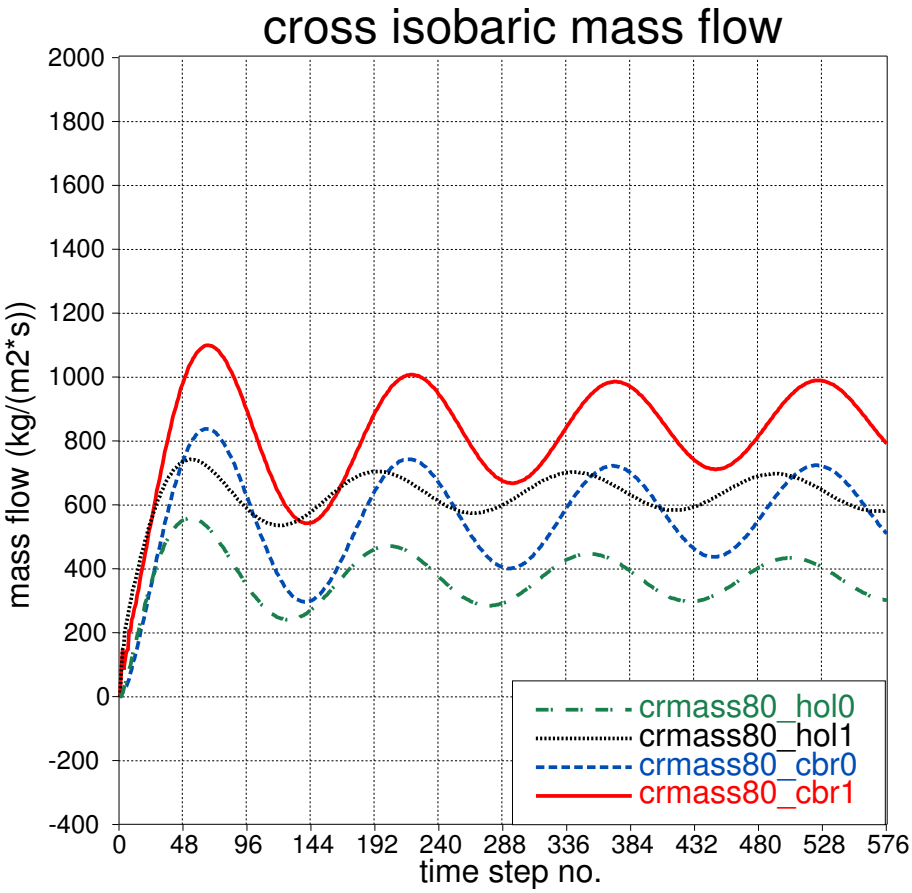

Colophone

Serial title:
Scientific Report 04-07

Title:
Rotation of the surface stress as a tool in parameterization of atmospheric turbulence

Subtitle:

Authors:
Niels Woetmann Nielsen and Bent H. Sass

Other Contributers:

Responsible Institution:
Danish Meteorological Institute

Language:
English

Keywords:
surface stress, turbulence

Url:
www.dmi.dk/dmi/sr04-07

ISSN:
1399-1949

ISBN:
87-7478-509-5

Version:
211220-2004

Website:
www.dmi.dk

Contents

Resumé

I numeriske modeller for atmosfæren er det ofte vanskeligt at producere en realistisk "Ekman pumpning" i atmosfærens grænselag. En metode præsenteres, som giver mulighed for at optimere en given turbulensparametrisering med hensyn til Ekman pumpningen.

Det vises for et idealiseret barotropt grænselag, at en drejning af overfladestresset i urets retning (nordlige halvkugle) i forhold til overfladelagets vindretning fører til en forøgelse af den vertikalt integrerede strømning på tværs af isobarerne. En parametrisering af denne stress-drejning præsenteres og testes for barotrope og barokline forhold. Det vises for et 3-dimensionalt case med en cyklon over Østersøen, at opfyldningsprocessen påvirkes af den ny parametrisering af overfladestresset. Begrænsningerne for turbulensparametriseringer i brug diskuteres i lyset af den beskrevne metode til optimering af turbulensskemaer.

Abstract

The production of a realistic ‘Ekman pumping’ in numerical models of the atmosphere poses a significant problem. A method is presented to tune a turbulence scheme of a given model to improve the behaviour of the boundary layer flow with respect to the Ekman pumping.

It is showm for an idealized barotropic boundary layer that a clockwise turning (northern hemisphere) of the surface stress with respect to the surface layer wind direction leads to an increased cross isobar mass flow in the boundary layer. A parameterization of such turning of the surface stress is presented and tested in 1-dimensional barotropic and baroclinic cases. It is shown for a 3-dimensional case that the parameterization can affect the filling of a decaying cyclone in the region of the Baltic Sea. The limitations of currently used turbulence parameterizations are discussed in the light of the present method to tune a turbulence scheme.

1. Introduction

A well known problem connected to cyclone prediction is how to describe the decaying cyclone correctly. The HIRLAM forecast model (Undén et al., 2002) has, as several other models, suffered from a too slow rate of filling of decaying cyclones. Basically, the filling of cyclones and weakening of high pressure systems is governed by frictional effects ('Ekman pumping') in the planetary boundary layer (referred to as PBL), that create a net mass flow across closed isobars in the PBL. The rate of filling of decaying cyclones depends on details of the applied parameterization of turbulence, including specification of boundary conditions. This makes it difficult to optimize a turbulence formulation to give the most realistic description of the turbulent friction in the atmosphere.

In the present report we describe the work done to achieve a better 'Ekman pumping' in the HIRLAM forecasting model applied at DMI. This model utilizes the CBR turbulence parameterization scheme, version 6.2.3, (Cuxart et al., 2000; Lenderink and Holtslag, 2004). The CBR scheme has a prognostic equation for turbulent kinetic energy (TKE) and a diagnostic, rather complex, calculation of the length scales utilized in the calculation of the shear, buoyancy, transport and dissipation terms in the TKE equation (Undén et al., Ch.3.5, 2002). The magnitude and direction of the surface stress, and hence the net horizontal ageostrophic mass flow in the PBL, depends on a number of parameters such as geostrophic wind, baroclinicity, surface roughness length and depth of the PBL. By experimentation, and not surprisingly, it has been found that the surface stress is sensitive to the way the lengths scales in the TKE equation are parameterized. This matter will only be briefly covered in the present report.

According to surface Rossby-number similarity theory the surface stress at a rigid surface is in the direction of the surface layer wind. However, this relationship is not universally valid. Over the ocean, where the surface stress has contributions from both wind and ocean waves, this rule is not generally valid [Grachev et al., 2004]. Measurements over the ocean in frontal zones have shown that the surface stress in the Northern Hemisphere is turned clockwise on the warm side and anticlockwise relative to the surface wind on the cold side of cold fronts [Persson et al., 2004].

In the present article we will investigate the impact on the 'Ekman pumping' of a clockwise rotation (Northern Hemisphere) of the surface stress relative to the surface layer wind in case of a neutral or stably stratified surface layer.

Rotation of the surface stress away from the surface layer wind direction has been suggested by Tijm (2003). He investigated the effect of a clockwise turning of the surface stress by a fixed amount and found promising results for the period he studied. A tentative parameterization of the stress rotation as function of the surface layer Richardson number was suggested by Nielsen, 2004 and test results with this parameterization in 1-dimensional experiments against runs without this change has been reported in Sass and Nielsen (2004). In the same report, the modified formulation was shown to have the desired effect of more rapid filling in a case study of a decaying, rather small-scale, cyclone over Denmark.

In section 2 we give the theoretical background for the proposed rotation of the surface stress relative to the surface layer wind. This section includes derivation of basic equations (section 2.1), consideration of the typical variation of the barotropic surface cross isobar angle with stability (section 2.2) and a qualitative discussion of a possible influence of improper representation of baroclinicity effects in the turbulence parameterization (section 2.3). The surface stress rotation can be regarded as a modified lower boundary condition for the turbulence scheme. In section 3 we present a simple and tentative parameterization of the surface stress rotation. Section 4 summarizes results of 1-dimensional experiments with and without the stress-turning. Experiments performed

with 40 and 80 vertical levels, respectively, indicate that the response to the stress-turning is moderately dependent on vertical resolution in the considered range. In corresponding 1-dimensional experiments a stronger sensitivity is found to the type of turbulence parameterization scheme in use. This is demonstrated by comparing runs using the CBR scheme with runs using a simpler first order closure scheme (the Holtslag scheme, Nielsen, 1998). Finally, section 5 contains discussion and conclusions.

2.1. Theory

Calculation of the surface stress in the HIRLAM model is based on Monin-Obukhov similarity for the barotropic, stationary and horizontally homogeneous surface layer. In these conditions the horizontal momentum equations simplifies to

$$0 = f(v - v_{g0}) - \frac{\partial \overline{u'w'}}{\partial z} = f v_a + F_x \quad (1)$$

$$0 = -f(u - u_{g0}) - \frac{\partial \overline{v'w'}}{\partial z} = -f u_a + F_y, \quad (2)$$

where $\vec{F} = (-\partial/\partial z(\overline{u'w'})\vec{i} - \partial/\partial z(\overline{v'w'})\vec{j})$ is the turbulent frictional force, $\vec{\tau} = (-\overline{u'w'}\vec{i} - \overline{v'w'}\vec{j})$ is the kinematic Reynolds stress, $\vec{V_{g0}} = u_{g0}\vec{i} + v_{g0}\vec{j}$ is the geostrophic wind and $\vec{V} = u\vec{i} + v\vec{j}$ is the mean wind velocity. A primed variable denotes deviation from the mean. The lower boundary condition (for $z = z_0$) is $\vec{V} = \vec{0}$ or $\vec{V_a} = -\vec{V_{g0}}$, yielding

$$f v_{g0} = -\frac{\partial \overline{u'w'}}{\partial z}_s \quad (3)$$

$$-f u_{g0} = -\frac{\partial \overline{v'w'}}{\partial z}_s, \quad (4)$$

where subscript s means the surface. Vertical integration of (1) and (2) over the depth, h, of the PBL with the assumption $\tau(\vec{h}) = \vec{0}$ gives

$$\langle \vec{F} \rangle = f\vec{k} \times \langle \vec{V_a} \rangle = -h^{-1}\vec{\tau_s}. \quad (5)$$

This equation shows that $\langle \vec{F} \rangle$, the mean value of the turbulent frictional force in the PBL, is in the opposite direction of the kinematic surface stress $\vec{\tau_s} = (-\overline{u'w'_s}\vec{i} - \overline{v'w'_s}\vec{j})$ and perpendicular to $\langle \vec{V_a} \rangle$, the mean value of the ageostrophic wind in the PBL.

From (1) and (2), by subtracting $\partial/\partial y$ of (1) from $\partial/\partial x$ of (2), we derive the vorticity equation

$$0 = \vec{k} \cdot \nabla \times \vec{F} - f\nabla \cdot \vec{V_a} - \vec{V_a} \cdot \nabla f. \quad (6)$$

In (6) the last term tends to be at least 1 order of magnitude smaller than the other terms. Furthermore, the Boussinesq approximation implies $\nabla \cdot \vec{V_a} + \partial w/\partial z \approx 0$. Therefore (6) can be approximated by

$$0 = \vec{k} \cdot \nabla \times \vec{F} + f\frac{\partial w}{\partial z}. \tag{7}$$

By adding u multiplied with (1) to v multiplied with (2) we obtain the rate of work equation

$$0 = -f\vec{V} \cdot \vec{k} \times \vec{V}_a + \vec{V} \cdot \vec{F}. \tag{8}$$

Since $\vec{V}_{g0}$ and $\vec{V}_a$ are perpendicular to $\vec{k} \times \vec{V}_{g0}$ and $\vec{F}$, respectively, (8) can be rewritten as

$$f\vec{V}_{g0} \cdot \vec{k} \times \vec{V}_a = \vec{V}_{g0} \cdot \vec{F}, \tag{9}$$

stating that the work done per unit time by the horizontal pressure gradient force is equal in magnitude to the work done per unit time by the turbulent frictional force.

Vertical integration of (7) and (9) over the depth of the PBL above a level bottom surface yields

$$w(h) = f^{-1}\vec{k} \cdot \nabla \times \vec{\tau}_s \tag{10}$$

and

$$F_A = fV_{g0}|\langle\vec{V}_a\rangle| \cos\alpha_F = V_{g0}|\langle\vec{F}\rangle| \cos\alpha_F, \tag{11}$$

respectively. In (10) $w(h)$, which is the vertical velocity at the top of the PBL, is a measure of the net cross isobaric mass flow in the PBL. It is proportional to the vertical component of the rotation of the kinematic surface stress, or equivalently, proportional to the vertical component of the rotation of the mean frictional force. In (11) F_A is the mean rate of work done by the frictional force in the PBL, and α_F is the angle between $\vec{V}_{g0}$ and $-\langle\vec{F}\rangle$. From (5) and (11) we obtain

$$|\langle\vec{V}_a\rangle| \cos\alpha_F = \frac{1}{f \cdot h}|\vec{\tau}_s| \cos\alpha_F. \tag{12}$$

Since $|\langle\vec{V}_a\rangle| \cos\alpha_F$ is the mean ageostrophic wind in the direction perpendicular to $\vec{V}_{g0}$ the lhs of (12) is proportional to the net cross isobaric mass flow in the PBL. According to (12) the latter is proportional to the component of the surface stress along $\vec{V}_{g0}$.

In the surface layer of high surface Rossby number flows the Coriolis force is negligible compared to the horizontal pressure gradient force and the frictional force, implying a wind and stress direction that is approximately constant with height in this layer. It is a widely applied assumption, related to surface Rossby-number similarity (e.g. Garratt, 1992, Ch. 3.2.1), that the stress is in the direction of the wind in the surface layer. With this assumption $\alpha_F = \alpha_0$, where α_0 is the surface cross isobar angle, i.e. the angle between the surface layer wind and the geostrophic wind.

Suppose that $\vec{\tau}_s$ is not in the direction of the surface layer wind, but rotated by a constant angle $0 < |\Delta\alpha| < \alpha_0$ with respect to $\vec{V}_s$. In the Northern Hemisphere (NH) a clockwise and counter clockwise rotation of $\vec{\tau}_s$ relative to $\vec{V}_s$ increases and decreases the component of $\vec{\tau}_s$ along $\vec{V}_{g0}$, respectively. The net cross isobaric mass flow in the PBL increases and decreases correspondingly.

According to (10) the increase and decrease in the net cross isobaric mass flow must be connected with an increase and decrease in $|\vec{\tau}_s|$, respectively, since $|\nabla \times \vec{\tau}_s|$ is invariant to a rotation of the coordinate system.

The tendency for having a too weak 'Ekman pumping' in HIRLAM therefore might suggest a clockwise rotation in the model of $\vec{\tau}_s$ relative to $\vec{V}_s$. Such a rotation by an amount $0 < \Delta\alpha \leq \alpha_0$ leads to a new equilibrium with a surface stress $\vec{\tau}_{s_*}$ having an angle α_{F_*} relative to $\vec{V}_{g0}$ and a surface layer wind with a cross isobar angle $\alpha_{0_*} = \alpha_{F_*} + \Delta\alpha$. If F_A and F_{A_*} is the rate of work done by the frictional force before and after the surface stress rotation, respectively, we have $F_A = V_{g0}\tau_s \cdot h^{-1}\cos\alpha_0$ and $F_{A_*} = V_{g0}\tau_s \cdot h^{-1}\cos\alpha_F = V_{g0}\tau_{s_*} \cdot {h_*}^{-1}\cos\alpha_{F_*}$. From the latter two relations and the increase in $|\vec{\tau}_s|$ in response to the clockwise rotation we get

$$\frac{h_* \cdot \tau_s}{h \cdot \tau_{s_*}} = \frac{\cos\alpha_{F_*}}{\cos\alpha_F} < 1 \tag{13}$$

or, since $\alpha_{F_*} = \alpha_{0_*} - \Delta\alpha$ and $\alpha_F = \alpha_0 - \Delta\alpha$,

$$\alpha_{0_*} > \alpha_0, \tag{14}$$

showing that the surface layer wind has a larger cross isobar angle α_{0*} in the equilibrium obtained in response to the surface stress rotation. Generally, it must be expected that the response to a constant surface stress rotation angle, i.e. the adjusted equilibrium values τ_{s_*}, h_* and α_{0_*}, depends on the turbulence parameterization scheme in use. One-dimensional DMI-HIRLAM experiments with different turbulence parameterization schemes, presented in section 4, show such a dependence.

An intensification of the 'Ekman pumping' obtained by rotating the surface stress clockwise relative to the surface layer wind by an amount $0 < \Delta\alpha \leq \alpha_0$ may be considered as a compensation for weaknesses in details of the applied turbulence parameterization.

2.2. Typical variation of the barotropic surface cross isobar angle with static stability

Knowledge about the typical variation of the surface cross isobar angle can be obtained from the surface Rossby-number similarity relations. For the barotropic idealized PBL considered here they read (e.g. Garratt, 1992, Ch. 3.4)

$$k\frac{u_{g0}}{u_{*0}} = \ln\left(\frac{h}{z_0}\right) - A_1(\mu, R) \tag{15}$$

$$k\frac{v_{g0}}{u_{*0}} = -B_1(\mu, R)\cdot \mathrm{sign}(f) \tag{16}$$

where $u_{*0} = {\tau_s}^{1/2}$, $\mu = h/L$, L is the Monin-Obukhov stability parameter and $R = |f|h/u_{*0}$, i.e. the PBL height normalized by $u_{*0}/|f|$, the PBL scale height due to the Earth's rotation.

The equations are valid in a coordinate system with the x-axis in the direction of the surface layer wind. The similarity functions A_1 and B_1 are empirical functions to be determined by experiments.

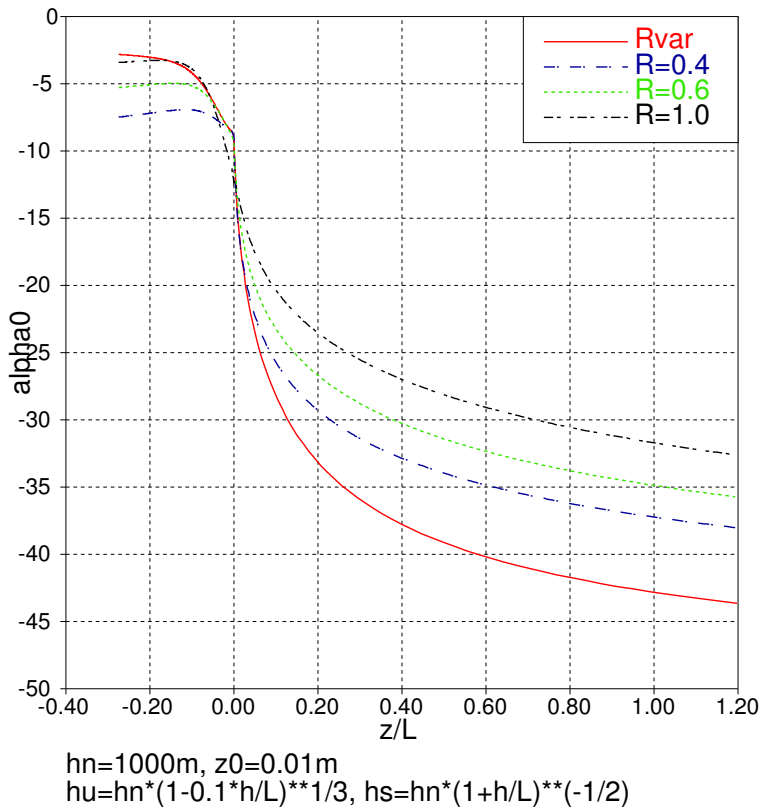

Figure 1: Variation of the surface cross isobar angle as function of z/L for a variable R_{var} (see text) and for R= 0.4, 0.6 and 1.0.

Uncertainty exists concerning the similarity functions. Arya (1977), has suggested the following approximations in the convective surface layer for the parameter ranges $R \geq 0.1$ and $-\mu \geq 2$

$$A_{1s} = \ln({\mu_*}^{1/2}) - 0.96{\mu_*}^{1/2} + 2.5 \quad (17)$$

$$B_{1s} = 1.15{\mu_*}^{1/2} + 1.1 \quad (18)$$

For the stably stratified surface layer Arya suggested for $\mu_* = R^{-1}\mu >> 1$ the approximation

$$A_{1u} = \ln(-\mu) + \ln R + 1.5, \quad (19)$$

$$B_{1u} = kR^{-1} + 1.8R\exp(0.2\mu). \quad (20)$$

In order to obtain a continuous formulation from the unstable to the stable regime we utilize the following rather ad hoc modifications to equations (17) to (20)

$$\bar{A}_{1u} = \ln\left(\frac{1}{1-\mu} - \mu\right) + \ln R + 1.5 \quad (21)$$

$$\bar{B}_{1u} = B_{1u}, \quad (22)$$

$$\bar{A}_{1s} = \ln\left(\left(\frac{1}{1+\mu_*}+\mu_*\right)^{1/2}\right) - 0.96\left(\frac{1}{c_{\mu a}+\mu_*}+\mu_*\right)^{1/2} + 2.5, \quad (23)$$

$$\bar{B}_{1s} = 1.15\left(\frac{1}{c_{\mu b}+\mu_*}+\mu_*\right)^{1/2} + 1.1, \quad (24)$$

where the modified similarity functions are denoted by an overbar and $c_{\mu a} = (0.96/(1-\ln R))^2$ and $c_{\mu b} = (1.15/(kR^{-1}+1.8R-1.1))^2$ are functions of R. From (15) and (16) follows

$$\tan\alpha_0 = -\frac{B_1 \cdot \mathrm{sign}(f)}{\ln h/z_0 - A_1}. \quad (25)$$

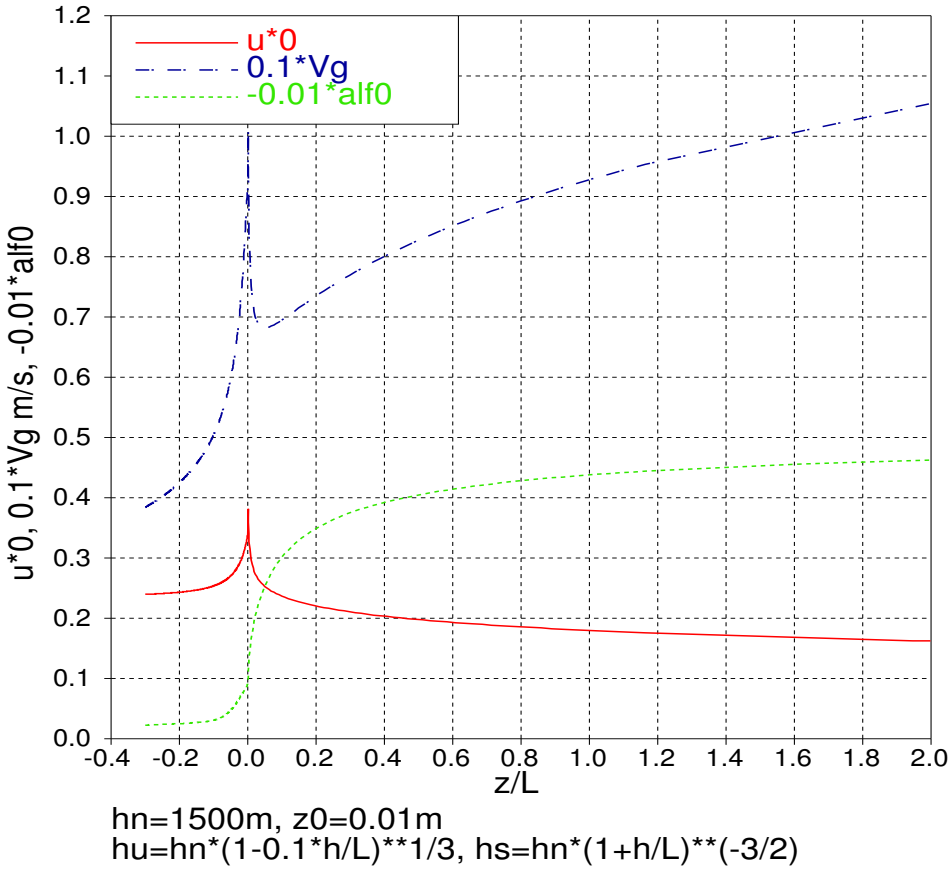

Figure 2: Surface friction velocity u_{*0}, surface cross isobar angle α_0 and geostrophic wind V_{g0} as function of z/L with the same parameter settings as for R_{var} in Figure 1. Note that V_{g0} and α_0 have been scaled by 0.1 and -0.01, respectively.

Figure 1 shows α_0 as function of $z/L = \mu h/z$ (z=10 m) for different values of R with the external parameter settings z_0=0.01, h_n=1000 m, $h_u = h_n(1-0.1\mu)^{1/3}$ and $h_s = h_n(1+\mu)^{-1/2}$ for R=0.4, 0.6 and 1, but with $h_s = h_n(1+\mu)^{-3/2}$ for $R = R_{var}$. The parameters h_u, h_n and h_s are the PBL heights in the unstable, neutral and stable boundary layer, respectively. Figure 1 shows that α_0 is sensitive to variations in R, particularly in stable stratification. In neutral stratification reported values of R are typically in the range 0.3 to 0.5. In the barotropic, unstably stratified PBL R is expected to increase with increasing $-z/L$ for a constant value of V_{g0}. In the barotropic, stably stratified PBL the following equilibrium boundary layer height, h_E, has been suggested [Zilitinkevich and Baklanov, 2002]

$$h_E = C_R \frac{u_{*0}}{|f|}\left(1 + \frac{C_R^2 C_{uN}}{C_S^2}\mu_N + \frac{C_R^2}{C_S^2}\mu_*\right)^{-1/2}, \tag{26}$$

where $\mu_N = N|f|^{-1}$, N is the free flow Brunt Vaisala frequency, $C_R \approx 0.5$, $C_S \approx 0.6$ and $C_{uN} \approx 0.3$. Equation (26) shows that R decreases with both increasing stability (μ_*) and increasing free flow stability (μ_N). If the free flow contribution is neglected (i.e. if only nocturnal PBL's capped by a residual layer is considered), it follows from (26) that

$$R = 2C_S^2\left(\mu + \sqrt{\mu^2 + 4(\frac{C_S^2}{C_R})^2}\right)^{-1}. \tag{27}$$

For the curve with label R_{var} in Figure 1, R is given by (27) in stable stratification and by $R = C_R(1-0.3\mu)^{1/3}$ in unstable stratification.

In the idealized barotropic, stably stratified surface layer above a rigid surface with $z_0 = 0.01\,m$ and $V_{g0} \approx 10\,\mathrm{ms}^{-1}$, -$\alpha_0$ is expected to follow, more or less, the curve with label $alf0$, shown in Figure 2. This figure also shows V_{g0} and u_{*0} as functions of z/L. The sharp peaks at $z/L = 0$ in u_{*0} and V_{g0} are created by the specific parameter settings in combination with the applied similarity functions in (21) to (24). If we compare with results of the 1-dimensional DMI-HIRLAM experiments, presented in section 4, we note significantly smaller modeled surface cross isobar angles in moderately to strongly stable stratification.

There are probably several reasons why turbulence schemes have difficulties in producing an Ekman pumping with the same space and time variation of intensity as in the atmosphere. It follows from the discussion given above that errors in the predicted direction and magnitude of the surface stress give rise to errors in the Ekman pumping. According to (15), (16) and (25) the surface stress direction is a function of the scaled PBL height, which means that errors in the predicted PBL height are associated with errors in the predicted surface cross isobar angle. Also, the assumptions of stationarity and horizontal homogeneity contribute to errors. Another limitation is the application of barotropic similarity relations in the parameterization of turbulence. In section 2.3 we discuss possible shortcomings due to this practice.

2.3. Effect of baroclinicity in the PBL

Consider a simplified baroclinic PBL with a thermal geostrophic wind varying linearly with height such that $\vec{V}_g(z) = \vec{V}_{g0} + \vec{S}_T z$, where $\vec{S}_T = S_{Tx}\vec{i} + S_{Ty}\vec{j}$ is a constant thermal wind shear and $\vec{V}_{g0} = V_{g0}\vec{i}$ is the surface geostrophic wind. The angle between $\vec{V}_{g0}$ and $\vec{S}_T$ is denoted by α_T and counted negative for warm advection.

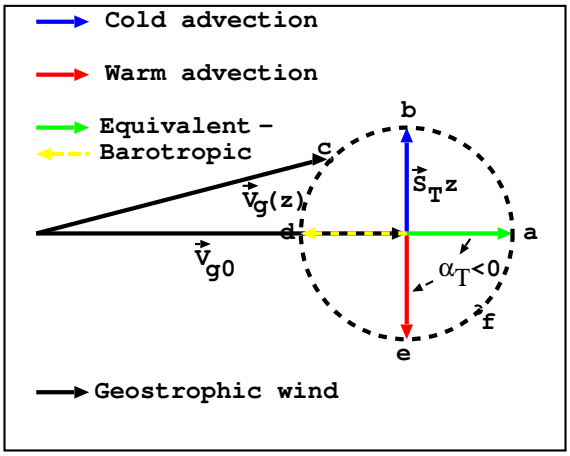

Figure 3: Variation of the geostrophic wind $\vec{V}_g$ with height in the PBL as function of the thermal geostrophic wind shear $\vec{S}_T$. The angle between $\vec{S}_T$ and $\vec{V}_{g0}$ is denoted α_T and counted positive in cold advection. $\vec{V}_{g0}$, having the arrow head at the center of the dashed circle is the surface geostrophic wind.

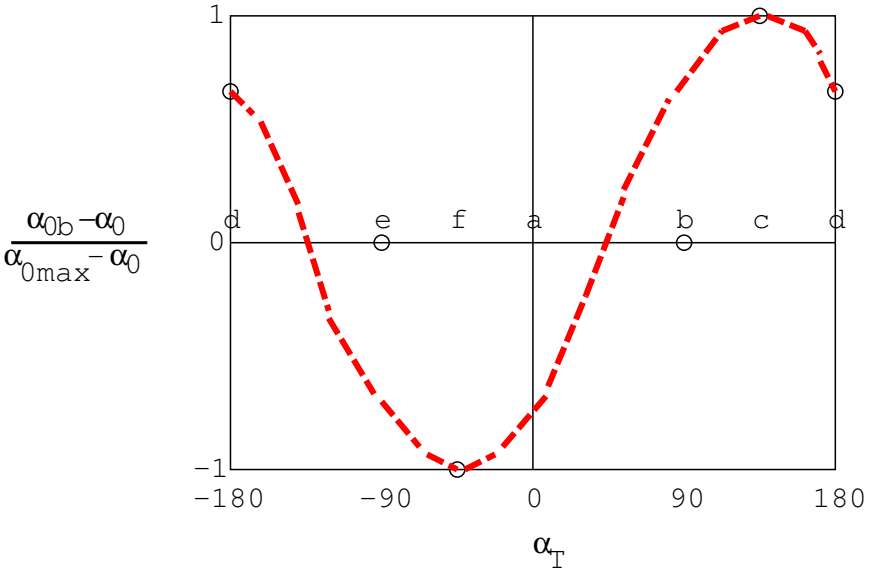

Figure 4: The dashed curve shows qualitatively the variation of the normalized difference $\alpha_0 - \alpha_{0b}$ with α_T, the angle between the thermal geostrophic wind shear and the surface geostrophic wind shown in Figure 3.α_0 and α_{0b} are the baroclinic and barotropic surface cross isobar angles, respectively.

We utilize Figure 3 as the basis for our qualitative, and not very precise, discussion of the effect of baroclinicity on the surface cross isobar angle α_0.

Consider a barotropic PBL with a geostrophic wind equal to the mean geostrophic wind $\vec{V}_{gm}$ (averaged over the depth of the PBL in Figure 3). The angle between $\vec{V}_{g0}$ and $\vec{V}_{gm}$ is denoted α_m and the surface cross isobar angle in the barotropic PBL with $\vec{V}_g = \vec{V}_{g0}$ is denoted α_0. According to

Figure 3, α_m has a maximum and a minimum in case b and e, respectively and $\alpha_m = 0$ in the equivalent barotropic cases a and d. The magnitude of $\vec{V}_{gm}$ has a maximum in case a and a minimum in case d. If α_{0m} is the surface cross isobar angle in the considered barotropic PBL (i.e. the angle between the surface layer wind $\vec{V}_s$ and $\vec{V}_{gm}$) and α_{0b} is the corresponding angle between $\vec{V}_s$ and $\vec{V}_{g0}$, we have $\alpha_{0b} = \alpha_{0m} + \alpha_m$. In the equivalent barotropic case a we expect $\alpha_{0b} < \alpha_0$, since the surface cross isobar angle decreases with increasing surface Rossby number $Ro = V_{gm}/(|f|z_0)$, where $V_{gm} = |\vec{V}_{gm}|$ and z_0 is the surface roughness length for momentum. From a to b the magnitude of $\vec{V}_{gm}$ decreases monotonically, implying a monotonic increase in α_{0m}. At the same time α_m increases to a maximum in case b. Consequently, α_{0b} increases monotonically from case a to case b. From case b to case d, α_m decreases to zero, while α_{0m} continues to increase, since $|\vec{V}_{gm}|$ continues to decrease. In cases near b the change in α_m is at a minimum, whereas the change in $|\vec{V}_{gm}|$ is at a maximum. For this reason the maximum in α_{0b}, referred to as α_{0max}, is expected to occur in cases near c in Figure 3. Similar arguments give as result that the minimum in α_{0b}, referred to as α_{0min}, is expected to occur in cases near f in Figure 3. Due to the circular symmetry we expect $\alpha_{0max} - \alpha_0 = -(\alpha_{0min} - \alpha_0)$.

The result of the discussion is summarized in Figure 4. This figure shows qualitatively the variation of $(\alpha_{0b} - \alpha_0/(\alpha_{0max} - \alpha_0)$ with α_T. The result is in fair qualitative agreement with observations [Mendenhall, 1967] and analytic model results [Wiin-Nielsen, 1974]. For high surface Rossby number flows the amplitude of $\alpha_{0b} - \alpha_0$ is expected to increase with increasing baroclinicity (i.e. increasing $|\vec{S}_T|$), since, for example, α_{0b} becomes smaller and larger in case a and case b, respectively. Note that in the baroclinic PBL the appropriate geostrophic wind in Ro becomes V_{gm} or $V_{g0} + \Delta V_g$, where ΔV_g is the change in magnitude of the geostrophic wind across the PBL. If $V_{g0} << \Delta V_g$ it becomes important to use this generalized definition of Ro. For an equilibrium baroclinic PBL with $V_{g0} << V_{gm}$ the qualitative discussion predicts $\alpha_{0b} = \alpha_c > 0$, independent of α_T. In section 4.1 we show that this prediction is in agreement with 1D experiments applying the CBR turbulence scheme, except for the sign of α_c. When applying the Holtslag scheme a similar result is obtained for the warm advection case e in Figure 3. In the other cases (a, b and d) turbulence does not develop near the surface. These contradicting results indicate either that the qualitative arguments become invalid in the baroclinic PBL with $V_{g0} << V_{gm}$, or that the applied turbulence parameterization gives an erronous response in these cases.

The discussion given here does not answer the question how stability (in terms of for example the Richardson number Ri) influences the amplitude of $\alpha_{0b} - \alpha_0$.

Figure 4 shows that the similarity functions in (15) and (16) for the baroclinic PBL also depend on the thermal geostrophic wind shear $\vec{S}_T$. Furthermore, due to the additional geostrophic wind shear in the PBL the depth of the PBL is expected to increase. In neutral and stable stratification Zilitinkevich and Esau (2003), have suggested

$$h = h_E(1 + C_0\frac{S_T}{N})^{1/2}, \tag{28}$$

where h and h_E are the baroclinic and barotropic equilibrium PBL depths, respectively, S_T is the magnitude of the thermal geostrophic wind shear and C_0 is an empirical constant (≈ 0.67).

The generally too weak 'Ekman pumping' in HIRLAM may be due to shortcomings of the turbulence parameterization affecting both the barotropic and the baroclinic PBL. Further discussion on this is postponed to section 4.

3. Parameterization of the surface stress rotation

After a rotation of the surface stress by an angle α the new components τ_{sx} and τ_{sy} of the surface stress may be expressed as follows in terms of the coordinates τ_x, τ_y for a stress vector in the direction of the lowest model level wind.

$$\tau_{sx} = \tau_x \cos\alpha + \tau_y \sin\alpha \cdot \mathrm{sign(f)} \quad (29)$$

$$\tau_{sy} = -\tau_x \sin\alpha \cdot \mathrm{sign(f)} + \tau_y \cos\alpha. \quad (30)$$

In (29) and (30) $\mathrm{sign(f)}$ is either 1 or -1 depending on the sign of the Coriolis parameter f. Let $\Delta\tau$ be defined such that

$$\tau = \Delta\tau + \tau\cos\alpha, \quad (31)$$

where $\tau = \left(\tau_x^2 + \tau_y^2\right)^{1/2} = \left(\tau_{sx}^2 + \tau_{sy}^2\right)^{1/2}$ is the magnitude of the surface stress. The problem is now to determine α. It follows from(31) that

$$\cos\alpha = 1 - \frac{\Delta\tau}{\tau}. \quad (32)$$

The following parameterization of $\Delta\tau$ is suggested. Assume that $\Delta\tau$ can be written as a function of a bulk Richardson number Ri_* for the lowest model layer, i.e.

$$\Delta\tau = \tau(1 - S(Ri_*)). \quad (33)$$

where

$$Ri_* = Ri + Ri_0$$

Ri is the conventional bulk Richardson number computed for the lowest model layer. Ri_0 is the value of Ri, above which the surface stress rotation is activated. A small positive value of Ri_0 means that the parameterization described below will be effective not only in the stable PBL, but also marginally into the unstable PBL. With equation (33) for $\Delta\tau$ we get

$$\cos\alpha = S(Ri_*). \quad (34)$$

The suggested functional form of S for $Ri_* \geq 0$ is

$$S(Ri_*) = 1 - \left(\frac{Ri_*}{1 + a \cdot Ri_*}\right)^{\gamma} \quad (35)$$

where

$$a = (1 - a_0)^{-1/\gamma} \quad (36)$$

It is expected that the optimal values for the parameters γ, a_0 and Ri_0 depend on the applied turbulence parameterization scheme. It is estimated (based on 1-D experiments) that $0.5 \leq \gamma \leq 1$. In the experiments described in section 4 the parameter settings were $\gamma = 0.5$, $a_0 = \frac{\sqrt{2}}{2}$ (corresponding to an asymptotic maximum rotation angle of $45°$) and $R_0 = 0.02$. The latter means that stress rotation was activated also in the marginally unstable PBL. The parameter values given above was chosen for illustrative purposes, and should not be considered as optimal values. For example was a_0 chosen to be at the very low end, with $a_0 = 0.9$ probably being closer to an optimal value.

4. Experiments

A number of 1-dimensional (1D) experiments has been performed with two different turbulence parameterization schemes, named HOL and CBR. The former is a K-closure scheme [Nielsen, 1998] and the latter has turbulent kinetic energy (TKE) as a prognostic variable (Cuxart et al., 2000; Lenderink and Holtslag, 2004). To show the effect of a clockwise rotation of the surface stress relative to the surface layer wind experiments have been performed with and without stress rotation.

The parameter settings applied in the parameterization of the stress rotation in the 1D experiments were $Ri_* = Ri + 0.02$ (see (35)), $\gamma = 0.5$ (see (35) and (36)) and $a_0 = \frac{\sqrt{2}}{2}$ (see (36)).

The initial conditions were specified as follows: A dry, barotropic atmosphere with a constant with height relative humidity of 20% and a geostrophic wind $V_g = 10\, ms^{-1}$, a surface temperature $T_s = 10°C$, a constant lapse rate of $0.009\, Km^{-1}$ up to 1500 m followed by isothermal conditions, and a bottom surface consisting of bare land with a roughness length $z_0 = 0.01\, m$. Runs were made at latitude $70°\ N$ from initial time 00 UTC on 20 December.

4.1. 1D experiments: Barotropic PBL

Figure 5 shows the effect on the surface cross isobar angle (α_0) and the cross isobaric mass flow (cmf) of (a): the applied turbulence scheme, (b): a change in the vertical model resolution and (c): a clockwise rotation of the surface stress relative to the surface layer wind. The surface cross isobar angle is calculated as the angle between $\vec{V}_N$, the lowest model level wind, and $\vec{V}_{g0}$. In the 40-level and 80-level versions the height of the lowest model level is approximately 35 m and 10 m, respectively.

The turbulence scheme HOL has a larger α_0 and a smaller cmf than the CBR scheme. In both schemes the response to an increase in the number of vertical levels from 40 to 80 is a small decrease in α_0 and a moderate decrease in cmf.

The response to a clockwise turning of the surface stress relative to the surface layer wind is an increace of α_0 and cmf in both schemes. In the 40 level versions the change in α_0 is largest in HOL (from about 30° to about 52°, whereas the relative increase in α_0 from 40 to 80 levels is largest in CBR. The decrease in cmf with vertical model resolution is largest in CBR.

Both with and without surface stress rotation the difference in performance prevails at very high resolution. This shows that the PBL in HOL and CBR evolve fundamentally different. Note in this context the phase lag (increasing with increasing vertical resolution) between the inertial oscillations of cmf in HOL and CBR and its (relatively weak) sensitivity to surface stress rotation.

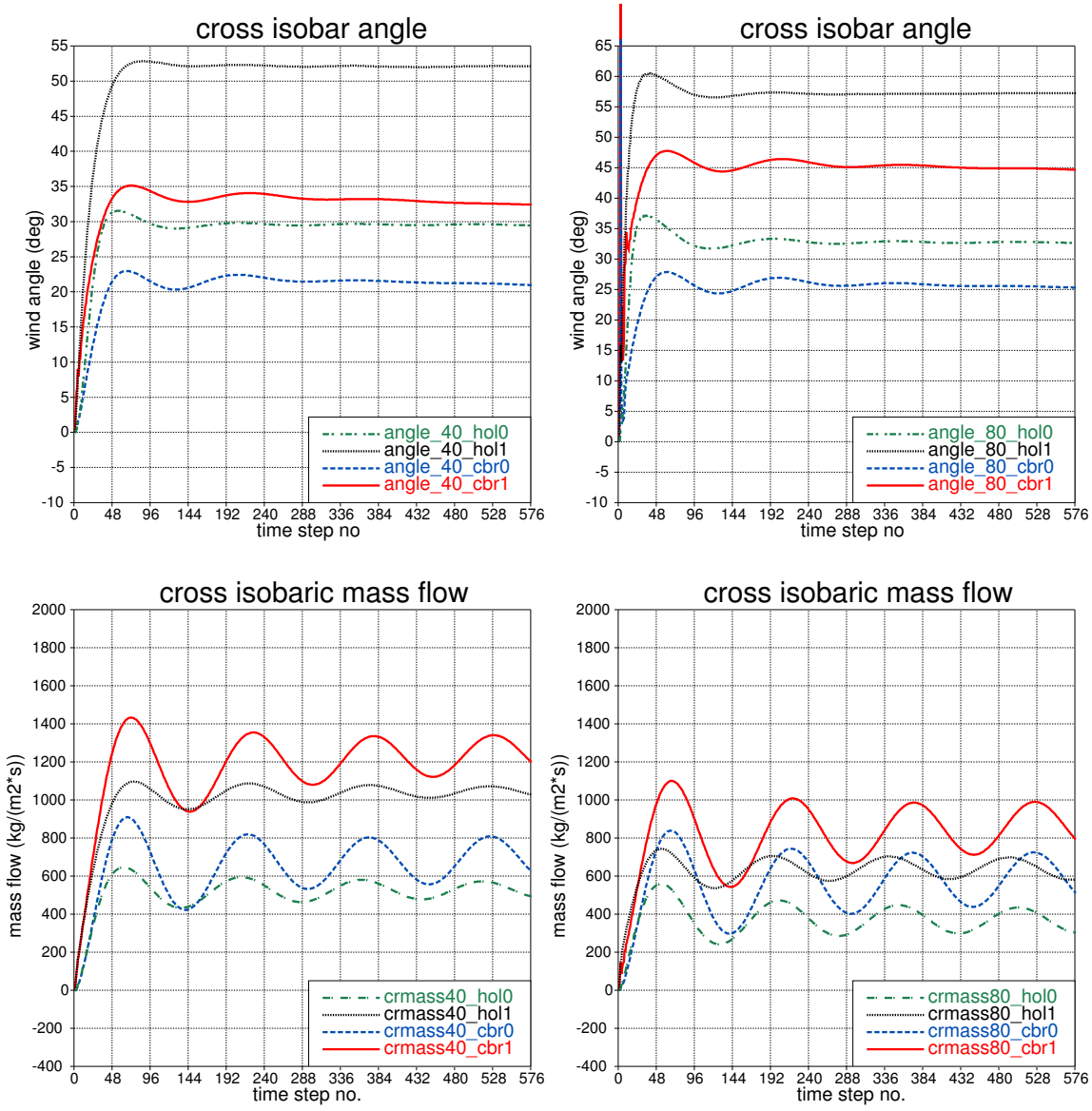

Figure 5: Variation with forecast lead time of surface cross isobar angle (top row) and cross isobaric mass flow (bottom row) in 1D-DMI-HIRLAM for barotropic conditions. Subscripts hol0 and cbr0 are for runs with the Holtslag scheme and the CBR scheme, respectively. Subscripts hol1 and cbr1 are for the same schemes with a clockwise rotation of the surface stress relative to the surface layer wind (see text). Subscripts 40 and 80 denote 40 and 80 vertical model levels, respectively. The location is at 70° N and the runs start from 00 UTC on 20 December with $z_0 = 0.01\,m$, $V_g = 10\,ms^{-1}$, $T_s = 10°\,C$ (surface temperature), a lapse rate $0.009 K m^{-1}$ up to 1500 m and isotermal conditions above. The initial relative humidity is 20% and constant with height. Time step 576 corresponds to 48 hours. Note the 4 inertial cycles in the cross isobaric mass flow and the more rapid damping of the corresponding oscillation in α_0.

The different evolution of the PBL is also shown by the vertical wind profiles in Figure 6. This figure shows different depths of the PBL, with a shallower PBL in HOL. The latter is consistent with lover values of cmf. The depth of the PBL increases with a clockwise rotation of the surface stress, consistent with the increase in cmf, shown by Figure 5. According to (28) baroclinicity in the neutral and stable PBL has a similar effect.

The positive impact of a clockwise rotation of the surface stress noted on verification against observation scores (Tijm, 2003; Järvenoja, 2004) might therefore be due to a compensation from the surface stress rotation to an improper representation of the effect of baroclinicity in the models, as discussed in sections 2.3 and 4.2.

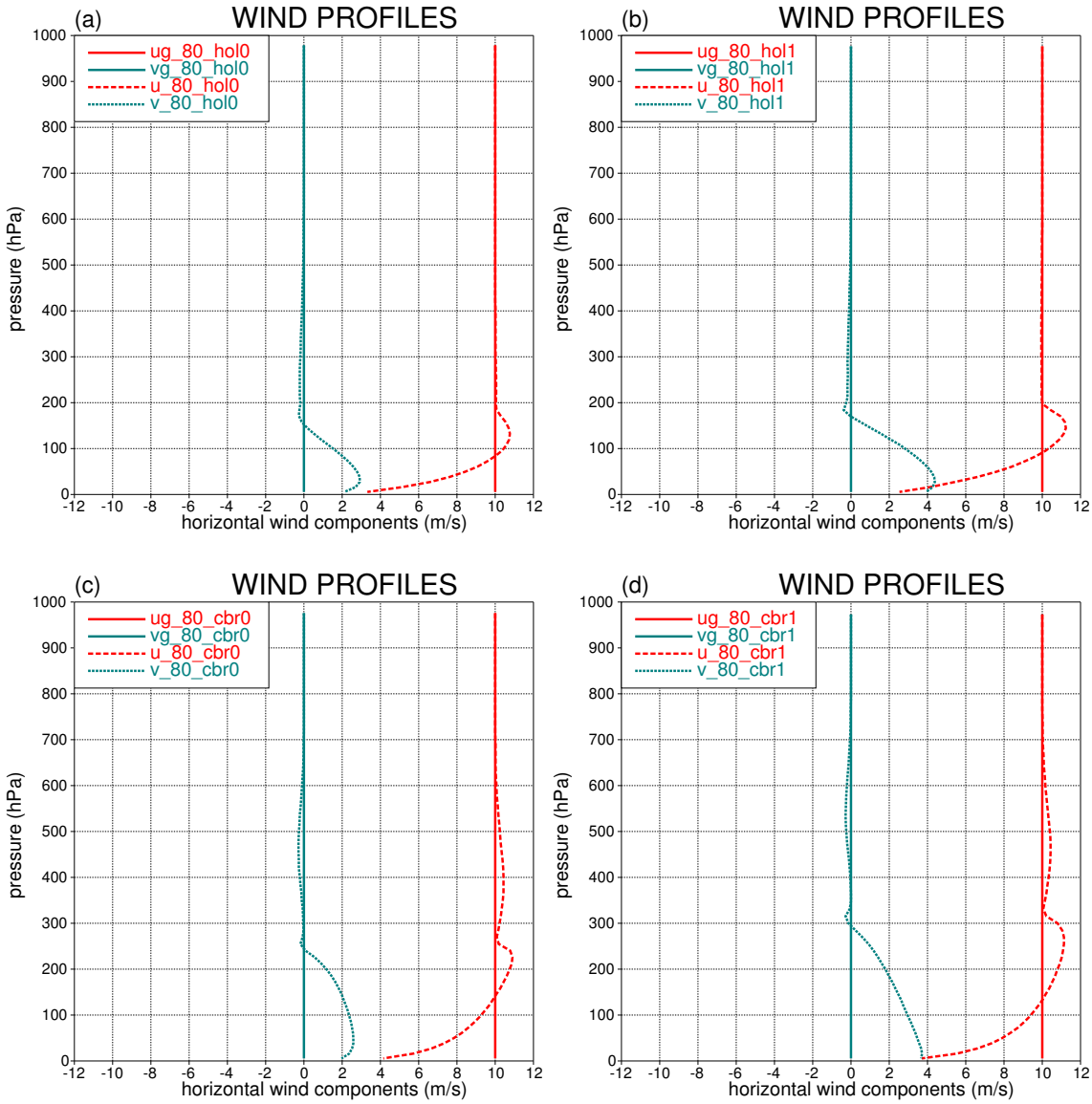

Figure 6: Vertical profiles of wind and geostrophic wind at 48 hour forecast lead time. Initial conditions and meaning of subscripts are the same as in Figure 5.

In section 2.1 it was shown that a clockwise rotation (NH) of the surface stress relative to the surface layer wind leads to a new equilibrium with an increased magnitude of the surface stress. This is confirmed by Figure 7, showing the time evolution of the magnitude of the surface momentum flux for HOL and CBR with and without rotation of the surface stress.

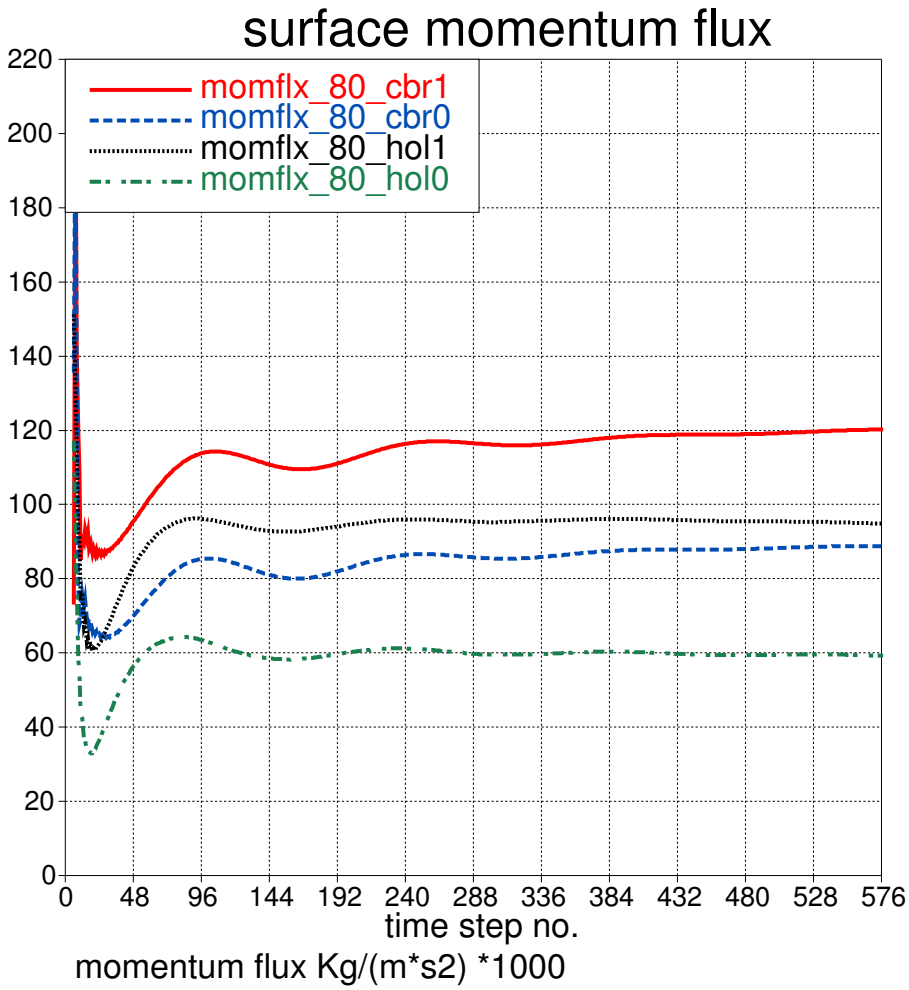

Figure 7: Evolution with time of the surface momentum flux. Initial conditions and meaning of subscripts are the same as in Figure 5.

4.2. 1D experiments: Baroclinic PBL

Results of 1-D experiments in a baroclinic PBL are shown in Figure 8 to 10. The initial conditions for the experiments are identical, except for V_{g0}, which changes from $10\,m\,s^{-1}$ in Figure 8 to $0.1\,m\,s^{-1}$ in Figure 9. The baroclinicity is prescribed as $|\vec{S}_T| = 5 \cdot 10^{-3}\,s^{-1}$. Following the convention in Figure 3, the angle between $\vec{V}_{g0}$ and $\vec{S}_T$ is $0°, 90°, 180°$ and $-90°$ in experiment names containing subscripts a, b, d and e, respectively. Experiment names with subscripts containing $hol0$ and $cbr0$ are without surface stress rotation, whereas $hol1$ and $cbr1$ are with surface stress rotation parameterized in the same way as in the barotropic experiments in section 4.1. The initial conditions are as in the barotropic experiments, except that the surface temperature is kept constant (10°C) with time in Figure 9 and allowed to cool to 0°C in Figure 8. As in the barotropic experiments the temperature in the atmosphere is changing with time due to advective and physical processes, including long wave radiative cooling.

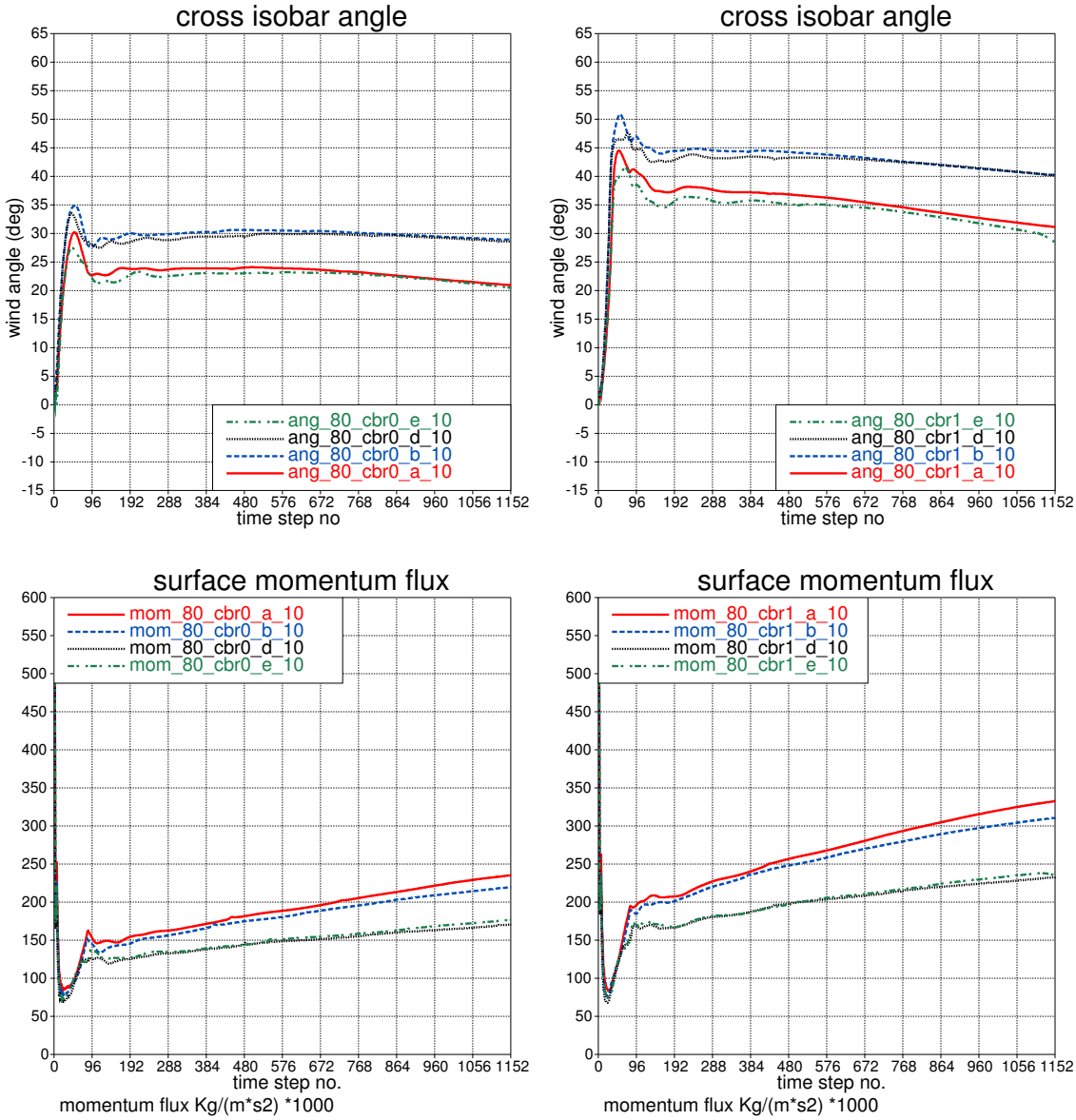

Figure 8: Variation with forecast lead time of surface cross isobar angle (top row) and the surface momentum flux (bottom row) in 1D-DMI-HIRLAM for baroclinic conditions with $V_{g0} = 10\,m\,s^{-1}$ and $|\vec{S}_T| = 5\,10^{-3}\,s^{-1}$. Left and right columns are without and with surface stress rotation, respectively, the latter as described in section 4. Initial conditions are as in Figure 4. The surface is only allowed to cool from $10°\,C$ to $0°\,C$.

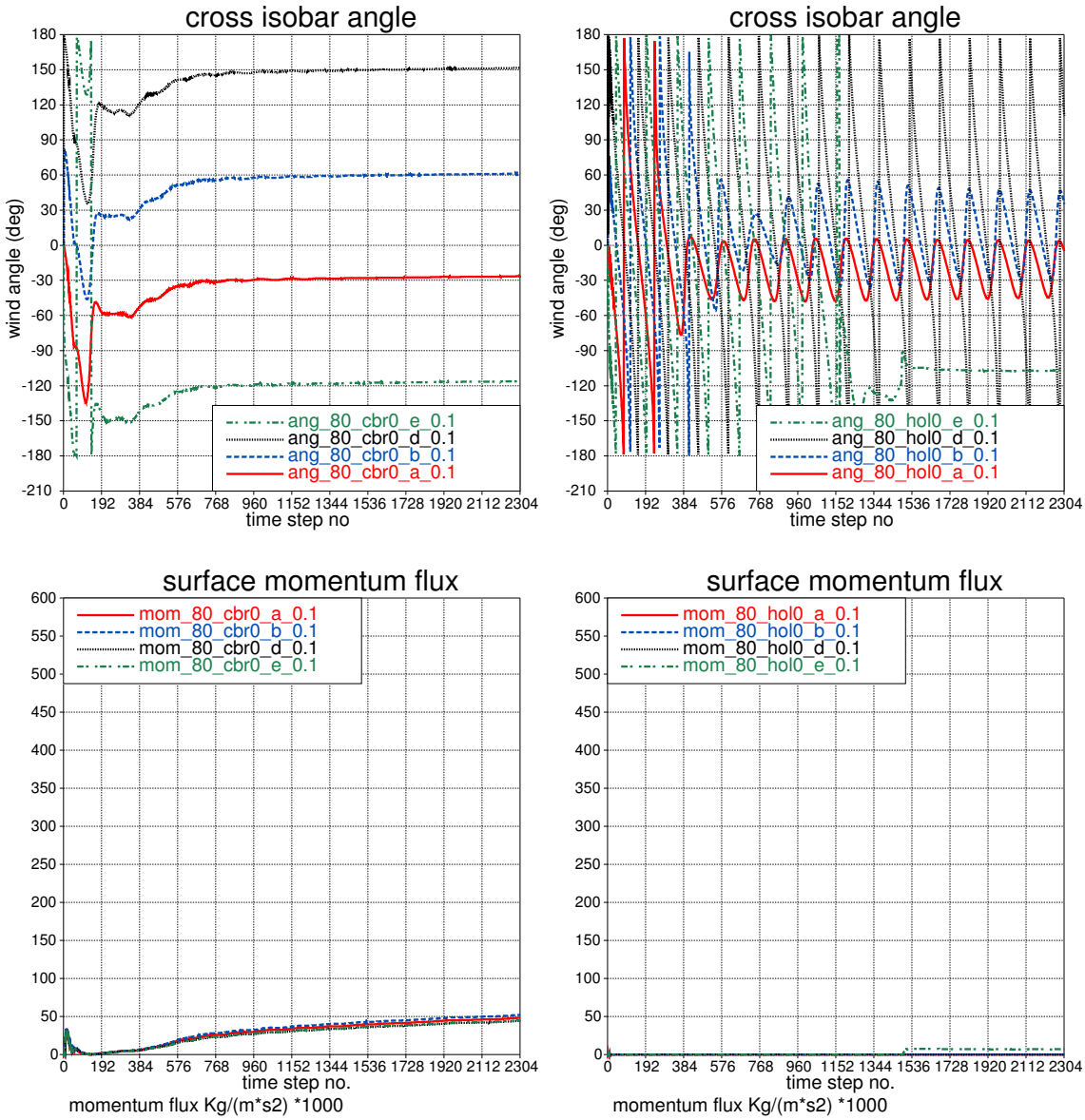

Figure 9: Variation with forecast lead time of surface cross isobar angle (top row) and the surface momentum flux (bottom row) in 1D-DMI-HIRLAM for baroclinic conditions with $V_{g0} = 0.1\,m\,s^{-1}$ and $|\vec{S}_T| = 5\,10^{-3}\,s^{-1}$. Left and right columns are with the CBR and the Holtslag scheme, respectively. No rotation of surface stress is applied. The initial conditions are as in Figure 4. The surface temperature is kept constant at $0^\circ\,C$.

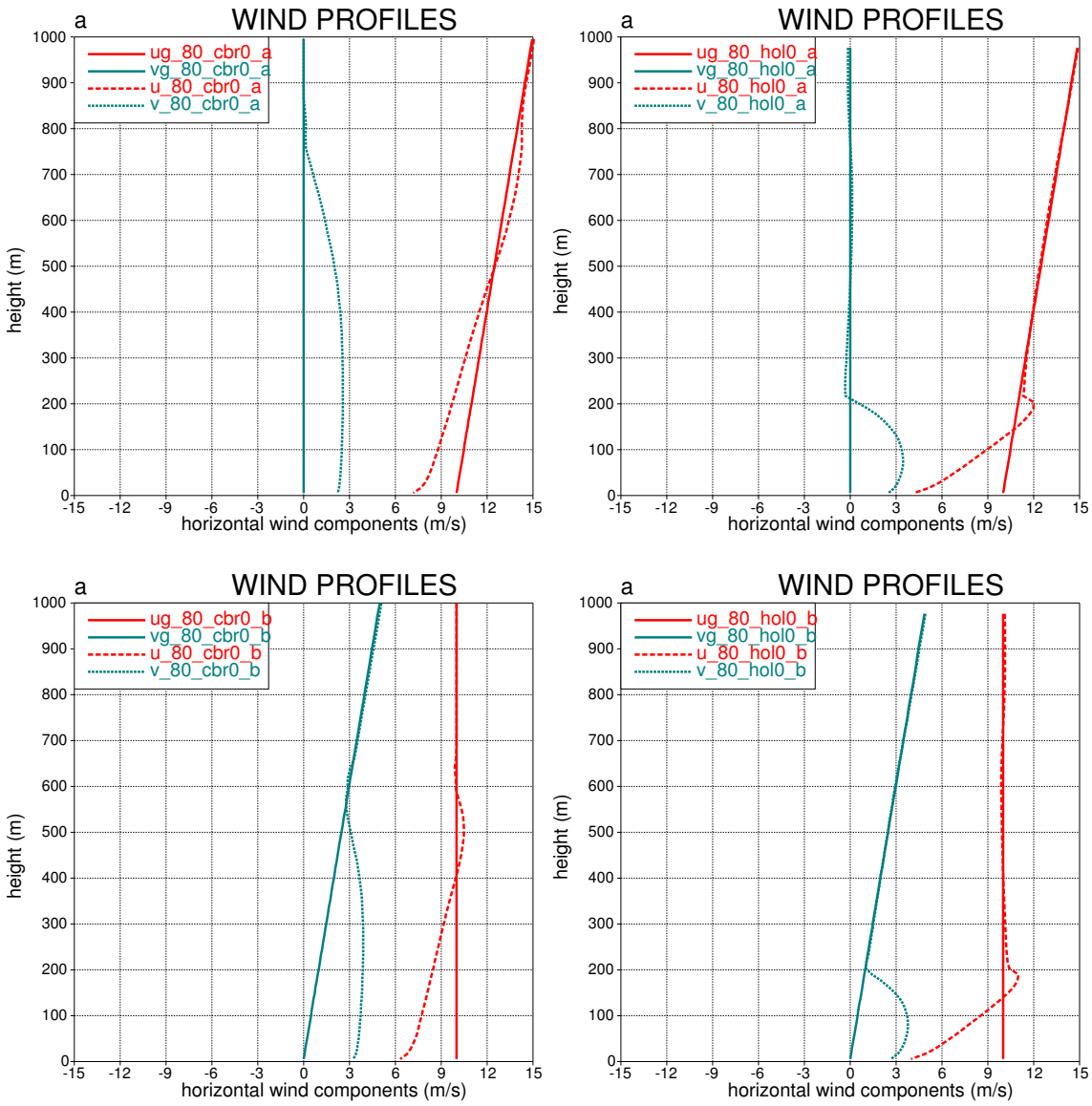

Figure 10: Vertical profiles of wind and geostrophic wind after 8 days (time step no. 2304). Left column is for the runs with subscript labels a and b in left column of Figure 8. Right column is for corresponding runs with the Holtslag scheme. No surface stress rotation has been applied.

Figure 8 shows the effect of baroclinicity on the surface cross isobar angle (upper row) and on the surface stress (bottom row) without (left column) and with (right column) surface stress rotation. Although the experiments are run out to day 4 (time step no. 1152), no equilibrium state was reached. By running a number of days further ahead in time a quasi equilibrium was reached. For certain values of α_T this quasi equilibrium was connected with transition to a PBL with stratocumulus below the PBL inversion (Figures not shown). Figure 8a and b (top row) are in qualitative agreement with Figure 4, showing that the turbulence parameterization at least to some extent is able to capture baroclinicity. The surface stress rotation increases α_0 by a little more than 10°, only weakly dependent on α_T. Figure 8c and d (bottom row) show that among the shown cases, τ_s is largest in case a and smallest in case d. The difference in τ_s between cases d and e is small, and the corresponding difference between cases a and b is relatively small. With surface stress rotation the amplitude of τ_s as function of α_T increases.

A similar series of 1D experiments were performed with the Holtslag scheme (figures not shown). Considerably less sensitivity to baroclinicity was found in these experiments.

A second series of 1D experiments were performed with a very low $V_{g0}(= 0.1\, m\, s^{-1})$, but unchanged baroclinicity S_T. The surface stress rotation was set to zero in these experiments. Figure 9 shows results for α_0 (top row) and τ_s (bottom row). Left and right columns show results with application of the CBR scheme and the Holtslag scheme, respectively. The response to baroclinicity is notably different. A quasi-stationary state with turbulence develops in runs with the CBR scheme, whereas this only happens in case e (warm advection by the geostrophic wind) in the experiments with the Holtslag scheme. Furthermore, the transition to turbulence occurs later and with a smaller surface stress (Figure 9, right column at bottom) and a smaller (negative) cross isobar angle $\alpha_{0m} \approx -15°$ (Figure 9, right column at top) in the latter experiment. Note that $\alpha_{0m} \approx -30°$ in the CBR runs, and thus nearly independent of α_T.

Figure 9 indicates that the vertical structure of the baroclinic PBL is significantly different in runs with the CBR and Holtslag schemes, respectively. The vertical wind profiles in Figure 10 show that this is indeed the case. The left column shows results with the CBR scheme in case a (top) and b (bottom), and the right column shows corresponding results with the Holtslag scheme. The initial conditions and parameter settings are as for Figure 8, left column. The Holtslag scheme has only weak sensitity to $\vec{S}_T$ and develops a shallow boundary layer, whereas the CBR scheme shows relatively strong sensitivity to baroclinicity. In the equivalent barotropic case (a) the CBR results show a 4 times deeper PBL than the Holtslag results. In the cold advection case (b) the PBL in the CBR runs is about 3 times larger. The different respose of the CBR and Holtslag turbulence parameterizations to both baroclinicity and surface stress rotation mainly originate from fundamentally different ways of calculating the mixing length.

The 1D experiments, presented in sections 4.1 and 4.2, show that a clockwise turning (NH) of $\vec{\tau}_s$ relative to $\vec{V}_s$ in both a barotropic and baroclinic PBL leads to a deeper PBL. In general, the baroclinic 1D experiments in section 4.2 do not answer the question about how realistic the model responds to baroclinicity. There is a clear indication of a too weak response in runs applying the Holtslag-scheme. The response to baroclinicity, in terms of α_0, appears to be more realistic in runs applying the CBR-scheme. In these runs the amplitude of α_0 as function of α_T is only weakly sensitive to surface stress rotation.

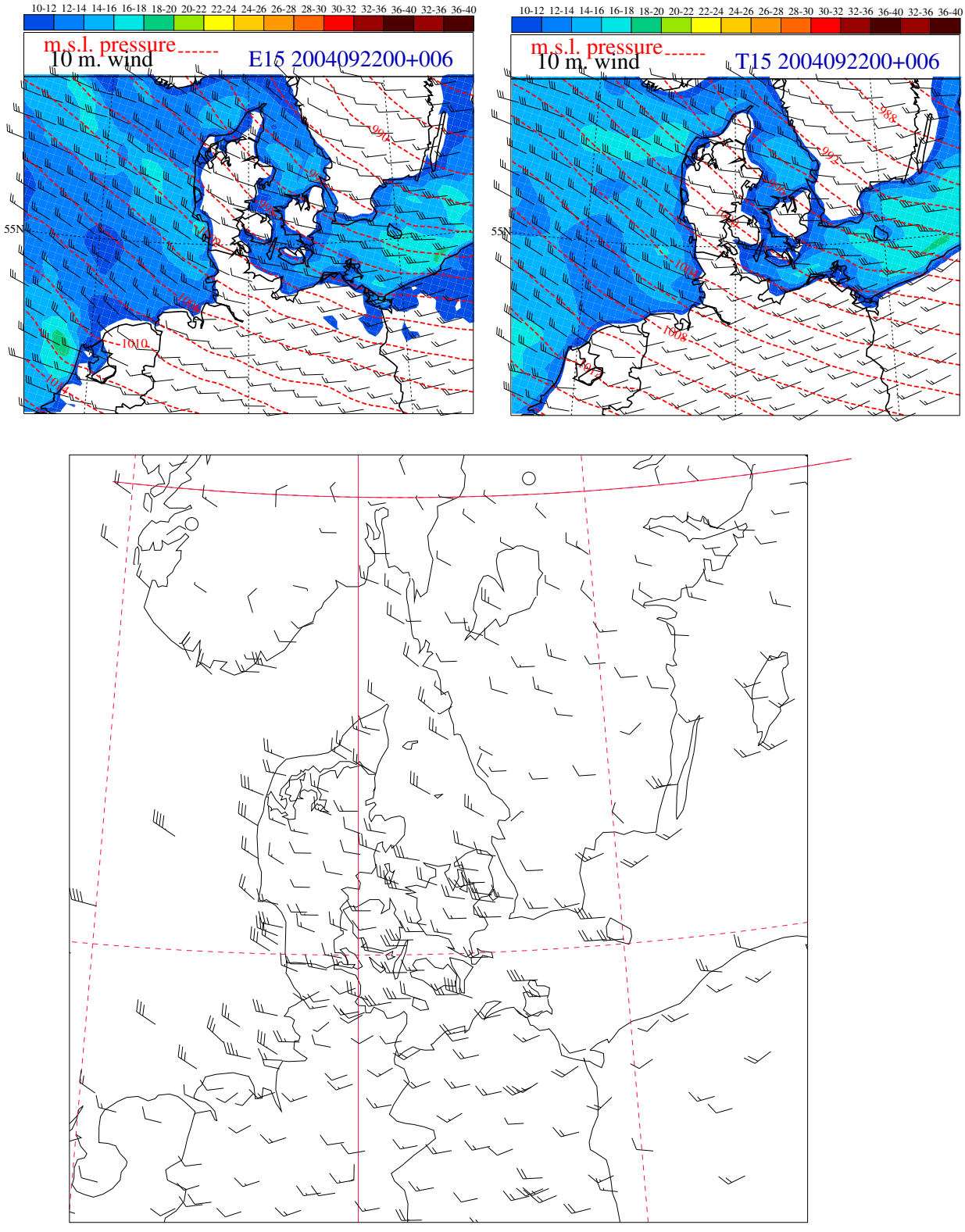

Figure 11: Upper row: 6 hour operational forecasts of mean seal level pressure (dashed curves) and wind velocity at 10m height, $V10m$ (color scale in ms^{-1}) valid at 00 UTC 22 September 2004. Left and right without and with surface stress rotation, respectively. Bottom: Observations of $V10m$ at valid time.

However, a clockwise rotation of the surface stress (related to larger α_0) has the effect of increasing the corresponding amplitude of the net cross isobaric mass flow. Consequently, with a clockwise rotation of the surface stress the "Ekman pumping' becomes relatively more efficient in cold advection (case b) and in particular in the equivalent barotropic case a (Figure 3 and 4). This is of interest, since mature synoptic scale systems tend to have an equivalent barotropic structure as in a with cold core cyclones and warm core anticyclones. With the introduction of clockwise surface stress rotation the decay of these systems progress faster. This is likely to be one among several reasons for the good results obtained in HIRLAM with a parameterization of surface stress rotation.

4.3. Operational forecasts

To give an impression of the impact of surface stress rotation on α_0 in real forecasts, Figure 11 shows operational DMI-HIRLAM forecasts of mean sea level pressure ($mslp$) and wind speed at 10m height ($V10m$). T15 and E15 are with and without surface stress rotation, respectively. In T15 the parameter settings in the parameterization of the stress rotation are different from those in the presented 1D experiments. The values are $Ri_* = Ri$, $\gamma = 1$ and $a_0 = 0.866$. The latter value forces the rotation angle of the surface stress relative to the surface layer wind asymptotically to 30° in the stable limit (for large Ri). Note that the rotation angle is counted positive for a clockwise rotation. The forecast lead time in Figure 8 is only 6 hours, which means that the differences in $mslp$ are small. Consequently, differences in $V10m$ between the two models are to a large extent due to the surface stress rotation applied in T15. Over land in T15 the surface layer wind $V10m$ is rotated counterclockwise relative to $V10m$ in E15, which means larger α_0 over land in T15. Significantly higher vegetation roughness lengths in T15 (3 times larger than in E15) also make a contribution to larger surface cross isobar angles in T15 in stable as well as unstable conditions.

5. Conclusions

We have studied an idealized barotropic PBL over a rigid surface. We have shown that a clockwise turning of the surface stress relative to the surface layer wind in the Northern Hemisphere intensifies the 'Ekman-pumping' by increasing the magnitude of the surface stress and the surface cross isobar angle.

The operational DMI-HIRLAM model suffers from a too slow filling of surface cyclones, which is a symptom of a weaker Ekman-pumping in the model than in the atmosphere.

We have suggested a parameterization of surface stress rotation with the aim of improving the performance of the Ekman-pumping in DMI-HIRLAM.

A number of 1D experiments have been presented with the main purpose of demonstrating the effect of the suggested parameterization on both the barotropic and baroclinic PBL. The experiments indicate that surface stress rotation can be used as a tool, compensating for weaknesses in the turbulence parameterization that generally results in a too weak Ekman pumping. The 1D experiments have shown that the response to a surface stress rotation in terms of magnitude of surface stress and net cross isobaric mass flow in both a barotropic and baroclinic PBL depends on the turbulence parameterization scheme in use. Particularly in the baroclinic PBL the response is much weaker with the Holtslag scheme than with the CBR scheme.

There may be several reasons for a weaker than observed Ekman-pumping in the model. Firstly, the applied turbulence parameterizations tend to give too small surface cross isobar angles (CBR) or a too shallow PBL (Holtslag) in stable stratifiation. Secondly, the parameterization of turbulence does not directly take into account influences of baroclinicity in the formulas relating turbulent surface

fluxes to prognostic parameters at the bottom and top of the lowest model half-layer. Theory as well as field observations suggest that surface layer similarity relations depend on baroclinicity. For example, the effect of baroclinicity on the surface cross isobar angle is to increase and decrease the angle during cold and warm advection, respectively. Another effect of baroclinicity is to increase the depth of the PBL. Based on 1D experiments in a baroclinic PBL we have presented arguments indicating that improper treatment of baroclinicity in the turbulence parameterization may contribute to an underestimation of the intensity of the Ekman-pumping, particularly in mature and decaying extratropical cyclones.

Thirdly, other factors, such as errors due to the assumptions of stationarity and horizontal homogeneity, errors arising from the parameterization of turbulence length scales (mixing and dissipation length scales) and related errors in prediction of the PBL height are also likely to contribute to errors in the Ekman-pumping.

Our present view is that a good functioning turbulence parameterization scheme has a minimum need for tuning, such as rotation of the surface stress. The presented one-dimensional experiments indicate that increased vertical resolution does not eliminate the need for optimization of the CBR sceme used in DMI-HIRLAM. Developing a more optimal turbulence parameterization might require fundamental changes of the parameterization. Until this has been achieved the suggested parameterization of surface stress rotation is considered to be an efficient (and simple) approach.

Acknowledgement

This work has been supported by EU project "Honeymoon", Contract no. ENK5-CT-2002-00606-HONEYMOON.

References

[Arya, 1977] Arya, S. (1977). Suggested revisions to certain boundary layer parameterization schemes used in atmospheric circulation models. *Mon. Wea. Rev.*, 105:215–227.

[Cuxart et al., 2000] Cuxart, J., Bougeault, P., and Redelsperger, J.-L. (2000). A turbulence scheme allowing for meso-scale and large-eddy simulations. *Quart. J. Roy. Meteorol. Soc.*, 126:1–30.

[Garratt, 1992] Garratt, J. (1992). *The atmospheric boundary layer*. Cambridge University Press.

[Grachev et al., 2004] Grachev, A., Fairall, C., Hare, J., Edson, J., and Miller, S. (2004). Wind Stress Vector over Ocean Waves. *J. Phys. Oceanogr.*, 33:2408–2429.

[Järvenoja, 2004] Järvenoja, S. (2004). Experimentation with a modified surface stress. *Hirlam Newsletter*, 45:113–123.

[Lenderink and Holtslag, 2004] Lenderink, G. and Holtslag, A. (2004). An updated length scale formulation for turbulent mixing in clear and cloudy boundary layers. To appear in. *Quart. J. Roy. Meteor. Soc.*

[Mendenhall, 1967] Mendenhall, B. (1967). A Statistical Study of the frictional Wind Veering in the Planetary Boundary Layer. Atmos. Sci. Paper No. 116, Colorado State University, Fort Collins.

[Nielsen, 1998] Nielsen, N. W. (1998). The first order nonlocal vertical diffusion scheme in HIRLAM 4.1. *HIRLAM Newsletter*, 31:12–13.

[Nielsen, 2004] Nielsen, N. W. (2004). The DMI-HIRLAM prediction of the cyclone over Scandinavia on 6 December 2003. *DMI Technical Report*, 04-09:1–17.

[Persson et al., 2004] Persson, P., Walter, B., and Hare, J. (2004). Maritime differences between wind direction and stress: Relationships to atmospheric fronts and implications, paper 1.9.

[Sass and Nielsen, 2004] Sass, B. and Nielsen, N. (2004). Modelling of the HIRLAM surface stress direction. *Hirlam Newsletter*, 45:105–112.

[Tijm, 2003] Tijm, A. (2003). Different aspects of the cbr/clj. *Hirlam Newsletter*, 44:43–47.

[Undén, 2002] Undén, P. (2002). Hirlam-5 Scientific Documentation. *Hirlam Publication*, pages 1–144.

[Wiin-Nielsen, 1974] Wiin-Nielsen, A. (1974). Vorticity, divergence, and vertical velocity in a baroclinic boundary layer with a linear variation of the geostrophic wind. *Bound. Layer Meteor.*, 6:459–476.

[Zilitinkevich and Baklanov, 2002] Zilitinkevich, S. and Baklanov, A. (2002). Calculation of the height of the stable boundary layer in practical applications. *Bound. Layer Meteor.*, 105:389–409.

[Zilitinkevich and Esau, 2003] Zilitinkevich, S. and Esau, I. (2003). The effect of baroclinicity on the equilibrium depth of neutral and stable planetery boundary layers. *Quart. J. Roy. Meteor. Soc.*, 129:3339–3356.

Previous reports

Previous reports from the Danish Meteorological Institute can be found on:
http://www.dmi.dk/dmi/dmi-publikationer.htm